THEORETICAL AND EXPERIMENTAL ESTIMATES OF THE BRITTLE STRENGTH OF SOLIDS PRODUCED BY COMPACTION OF POWDERS

V. M. Kornev, A. G. Demeshkin, and T. A. Korneva [1]   UDC 539.375

The strength characteristics of pressed-powder compacts are obtained. The fractal structure of the compact samples is described. Complex thermal analysis shows that during compaction of dry powders, interatomic interaction is partially restored. Quantitatively estimates of the theoretical strength of the samples are obtained and a possible mechanism for the propagation of flat cracks is proposed.

Introduction. The fractal fracture of brittle solids has been the subject of much research (see [1–3] and the bibliography to them). Apparently, the formation of fractal fracture surfaces is related to the physical and chemical nature of particles. The original structure of particles arises during growth of polycrystals from melts or solutions [4] and also during aggregation of finely dispersed particles under the action of capillary forces [4, 5]. Below, it is shown that the original structure of the material is partially preserved during powder compaction, and, therefore, the characteristic size of incipient cracks in the compact is related to the dimensions of the fractal branches.

1. Compaction of $Al(OH)_3$ and $AlO(OH)$ Powders and Strength Characteristics of Compacts. Before compaction, the starting $Al(OH)_3$ powder was passed through a screen with a cell size of 0.05 mm. Microscopic examination showed that particles of the powder differed in size by an order of magnitude. The largest particles had cracks. The $AlO(OH)$ powder was precipitated from a solution in the form of separate clods, which were ground before being placed in a mould.

Compaction was performed in a mould shaped like a truncated cone with a slope angle of the generatrix of 1.5°. The height of the compact was about 9.1 mm. The density and compression strength were determined for samples compacted with various pressing forces. In Fig. 1, the points show results of full-scale tests: curves 1 and 2 for $Al(OH)_3$ and $AlO(OH)$ powders, respectively, are curves of the compression strength σ^* versus the pressing force p, and curves 3 and 4 for the same powders are curves of the compact density ρ versus the pressing force p. Here it is assumed that $\sigma^* > 0$. As shown in Fig. 1, in the range of compaction up to 1.5 GPa, the dependence of the compact density on the pressing force is rather weak, and the strength of the samples depends greatly on the pressing force and is nearly linear.

In compression test, the compacts were broken along the lines of slide: the bottom of a broken sample was as a rule a cone with generatrix of about 45°. Fracture originated from shear. The fracture surface had an irregular structure. Apparently, the final fracture surface obtained after breakup of the sample into parts is smoothed as compared to the initial fracture surface since sliding of these parts over one another led to chipping of certain particles protruding from the initial "averaged" fracture surface.

2. Description of the Structure of Compacts. Before compaction, the powders were examined with an ordinary microscope. It was noticed that particles of the $AlO(OH)$ powder were accumulated in fractal-type aggregates, and the smaller the particle size, the more intense the agglomeration (sticking) of particles [4, 5]. Figure 2 scales up photographs of $Al(OH)_3$ powder particles before compaction. The surfaces
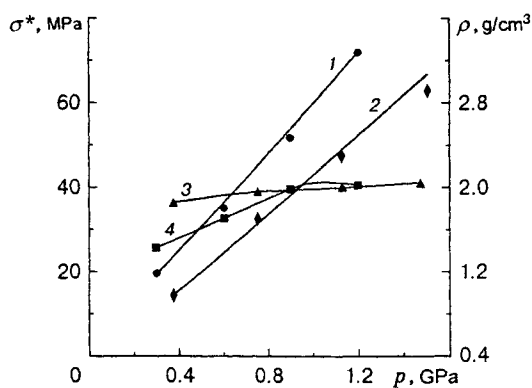
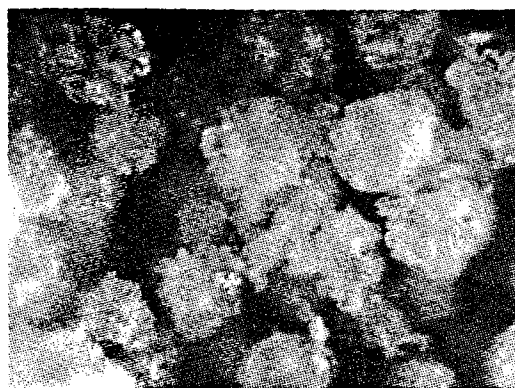Fig. 1   Fig. 2

of the Al(OH)$_3$ and AlO(OH) particles are severely dissected, and their structure resembles branches of spatial fractals. Thus, before compaction, the starting Al(OH)$_3$ and AlO(OH) powders had a certain structure.

It seems impossible to study the structure of the compacts directly because microsections of a compact cannot be prepared: the sample collapse in grinding. Therefore, a compacted Al(OH)$_3$ sample was placed in a special grain and covered with epoxy resin. After solidification of the resin, a microsection was prepared from the strongest part of the modified sample. The microsection was then observed through a microscope of 600 power. Different segments of the microsection had nonuniform structures and a random texture. The clotted aggregates have nonhomogeneous, diffused edges, which are hidden in the cement (epoxy resin), and, sometimes, separate grains are visible. Orientation of the particles is absent. The grains frequently form branching, dendritic fractal-type structures with discontinuous, loosely bound, or even completely broken branches, which can be treated as incipient cracks. This structure of the material indicates that the compact was produced by pressing. Stronger segments stand apart from less strong segments, and they variously react to compression, becoming random conglomerates of pressed and crumbled fractals immersed in the ambient mass.

Thus, it can be argued that the original structure is not completely destroyed in compaction. Therefore, the size of the incipient cracks is related not only to the grain size but also to the typical dimension of the fractal branches before compaction.

We describe the compaction process from the viewpoint of pressing of the fractals. In additional loading, separate grains and incipient fractals first merge, and a certain brittle solid skeleton of the starting compact forms. Then, with increase in the compression load, separate branches of the fractals break off and fill the "pockets" available in the skeleton of the starting compact. This should slightly increase the density of the sample, as is observed in the experiment (see Fig. 1). In addition, when the "pockets" are filled, the length of the critical crack decreases and the strength of the sample should increase (see Fig. 1).

3. Re-Establishment of Interatomic Interactions along Contact Surfaces in Compaction of AlO(OH). In composition, the examined sample is a hydrated modification of aluminum hydroxide AlO(OH), which is most similar in properties to the amorphous aluminum hydroxide synthesized and studied by Sato [6]. It should be taken into account that in comparison to the theoretical strength, the compaction pressure is low (differs by orders of magnitude). Therefore, one might expect that in powder compaction, only rather weak interatomic interactions can be restored. Partial restoration of these weak bonds was reliably detected in a physical experiment.

We performed a comparative study of AlO(OH) samples (powder and pellets) by complex thermal analysis. The essence of the method is that during heating of a sample under a particular program, the following characteristics are recorded: (1) endo- and exothermic reactions occurring in the sample (the sample temperature changes compared to the reference ΔT); these reactions are represented by a qualitative curve of differential-thermal analysis (DTA); (2) the change in the sample weight (Δm) as a function of the temperature [thermogravimetric (TG) curve]; (3) the rate of change in the sample weight with time dm/dt as a function

963

$\frac{dm}{dt}$, ΔT

DTG

DTA

TG

Δm, mg

0

20

40

60

14.8%   15.7%
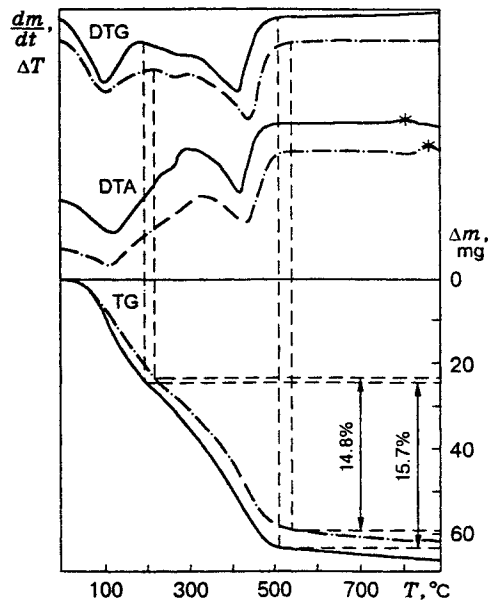
100   300   500   700 T,°C

Fig. 3

of the temperature [qualitative differential thermogravimetric (DTG) curve].

For comparison, we studied samples of two types: a powder sample and a compacted samples with a mass of 242 mg. Figure 3 shows TG, DTG, and DTA curves for aluminum hydroxide: the solid curves correspond to the powder sample, and the dot-and-dashed curves correspond to the pellet. In the experiment, the heating rate was $12°C \cdot min^{-1}$ and the maximum change in the sample weight was 100 mg. The powder sample is characterized by an endothermic effect (DTA curve), which reaches a maximum value at $110°C$ and is associated with removal of absorbed water, and a broad endothermic effect, which reaches a maximum value at $420°C$ and is attributed to removal of OH-groups. The weak endothermic effect observed at $270°C$ is due to the presence of small amounts of $Al(OH)_3$ in the sample. Bends on the DTG curve correspond to all endothermic effects. The amount of desorbed water is determined from the TG curve.

For the compact, maximum removal of OH groups takes place at $440°C$ (DTA curve in Fig. 3). The amount of desorbed water decreases from 15.7% for the powder sample to 14.8% for the compacts, and this clearly demonstrates partial restoration of interatomic interaction in the compacts. For the compact, constitution water is desorbed at higher temperatures. An exothermic effect due to phase transformation of the amorphous Al_2O_3 formed by decomposition of AlO (OH) to γ-Al_2O_3 is observed in the powder sample at $800°C$. For the compacts, it is shifted to $870°C$ and becomes more pronounced. These characteristic effects are denoted by asterisks on the corresponding curves. The indicated processes are the reverse to those observed in the mechanical activation of AlO (OH) [7].

4. Theoretical Estimates of Strength. We study the strength of a more or less real compact structure rather than of a regular packing of identical particles, as in [8]. We restrict our consideration to the most dangerous single cracks. The size of the compact particles differs by five orders of magnitude from interatomic distances. Therefore, to obtain estimates of the strength, we can restrict ourselves to a two-dimensional analysis. Two cases are considered: (1) the real interior crack is modeled by a sharp straight crack of equivalent length $2l$; (2) the real edge crack is modeled by a sharp edge crack of length l. A weak monolayer of atoms with defects is examined. (The characteristic of these defects are refined below.) To evaluate the brittle strength of a cracked body, we use the following two-dimensional discrete–integral criterion of brittle strength [8, 9]:

$$\frac{1}{kr_e} \int_0^{nr_e} \tau_{xy}(x,0)\, dx \leqslant \delta\tau_m. \tag{4.1}$$

Here τ_{xy} are the shearing stresses at the crack tip (these stresses act in the depth of the compacted material having an interior crack of length $2l$ or an edge crack of length l), Oxy is a rectangular coordinate system with coordinate origin at the crack tip, r_e is the characteristic distance between the centers of the atoms, n and k are numbers ($n \geqslant k$, where k is the number of acting interatomic bonds), nr_e is the interval of averaging, τ_m, $\delta\tau_m$ are the theoretical shear strengths for an ideal crystal lattice and an imperfect lattice, respectively, and δ is a parameter (we assume that $\delta = 1$ for an ideal crystal lattice and $\delta \leqslant 1$ for an imperfect lattice). The parameter δ describes the irregularities between individual grains of material in the crystal lattice restored. The introduction of the parameter δ is apparently justified if the contacting particles have an ideal structure, and imperfections are concentrated along grain boundaries. At the tip of the "sharp" crack there are vacancies [8], which are quite natural for bodies produced by powder compaction.

We dwell on the choice of the interval of averaging in relation (4.1). Let the particles (grains) have an ideal crystal structure. We believe that the most dangerous case is the presence of small-angle boundaries of such grains (see, for example, Fig. 7.3.3 in [10], where a small-angle boundary for a square two-dimensional lattice is shown schematically). Typical values of the constants are $k = 1$; $n_1 = 5, 6, \ldots, 12$, i.e., the linear dimension characterizing the periodic structure of small-angle boundaries is 5–12 times larger than the interatomic distance. The theoretical strength of such a material with a small-angle boundary of ideal grains can be estimated as follows: it is approximately 5–12 times smaller than the ideal shear strength [11] of a perfect crystal lattice τ_m, i.e., $\delta\tau_m \cong \tau_m/(5\text{-}12)$. The interval of averaging in the relation is calculated from the formula $n = n_1 n_2$, where $n_2 = 1$, 2, and 3. For $n_2 = 2$ or $n_2 = 3$, one or two "supervacancies" form on the small-angle boundary with one interatomic bond at the crack tip.

We assume the stress-free sides of the crack do not interact, although we consider cracked solids in compressions. This assumption is natural in view of the description of the compact structure (see Sec. 2).

We use the classical representation of the solution by the sum of smooth and singular components, the last of which is expressed in terms of the stress-intensity factor K_{II}:

$$\tau_{xy}(x,0) = \tau_\infty + K_{\mathrm{II}}/(2\pi x)^{1/2}, \tag{4.2}$$

where τ_∞ are the characteristic stresses of the problem considered. In our case (see Sec. 1), where the compression strength of the sample was studied, we have $\tau_\infty = \tau_{\max} = \sigma^*/2$. Taking into account (4.2) and performing obvious transformations, from criterion (4.1) we obtain the following relations for the critical stress-intensity factor K_{II}^*:

$$\frac{K_{\mathrm{II}}^*}{\tau_\infty} \leqslant \left(\frac{k\delta\tau_m}{n\tau_\infty} - 1\right)\left(\frac{\pi n r_e}{2}\right)^{1/2}, \qquad \frac{2K_{\mathrm{II}}^*}{\sigma^*} \leqslant \left(\frac{2k\delta\tau_m}{n\sigma^*} - 1\right)\left(\frac{\pi n r_e}{2}\right)^{1/2}. \tag{4.3}$$

For the first and second cases, the stress-intensity factors are calculated from the following formulas (see [12, pp. 44, 124]): $K_{\mathrm{II}} = 0.5\sigma(\pi l)^{1/2}$ and $K_{\mathrm{II}} = 0.364\sigma(\pi l)^{1/2}$, and the angle between the compressing stresses and the crack plane is $\pi/4$. Apparently, in the adopted notation, the greatest danger is introduced by interior cracks (the special conditions of fractal formation in the vicinity of a rigid wall are not studied here). Substituting (4.2) into the second relation of (4.3), we obtain the following simple expression for the critical length of the crack $2l^*(nk)$ with unit length r_e:

$$\frac{2l^*}{nr_e} = \left(\frac{k}{n}\frac{\delta\tau_m}{\sigma^*/2} - 1\right)^2. \tag{4.4}$$

We consider relations (4.3), (4.4) for the critical parameters: basically, they admit passage to the limits $K_{\mathrm{II}}^* \to 0$ and $2l^* \to 0$ (in the classical relation, this limiting transition is absent). The critical state of a body without a crack takes place when $k\delta\tau_m = n\sigma^*/2$, i.e., the average stresses are equal to the theoretical strength of the body with allowance for the really acting bonds in the structure considered.

Let the maximum linear dimension of the crack be of the order of ten maximum diameters of powder grains. Then, the estimate $2l^*/(nr_e) \cong 10^6$ holds. We calculated the critical stress as a function of the critical crack length [see relation (4.4)]. Figure 4 shows curves of the dimensionless critical stresses $(\sigma^*/2)/(\delta\tau_m)$ for two intervals of the critical crack lengths; the parameters $k = 1$ and $n = 10$ were used in the calculations. The
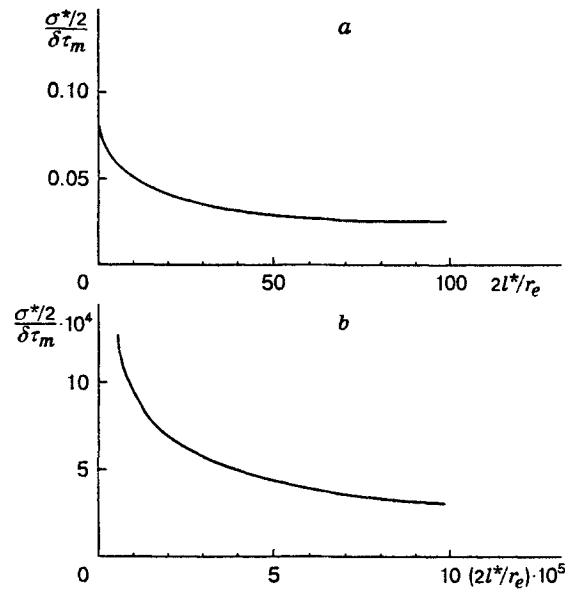
Fig. 4

first interval $0 \leqslant 2l^*/r_e \leqslant 100$ is of interest from the viewpoint of crack incipience, and the second interval $10^5 \leqslant 2l^*/r_e \leqslant 10^6$ describes the strength of the compacts. The obtained theoretical estimates (Fig. 4b) are in qualitative agreement with the results of full-scale experiment presented in Fig. 1. For qualitative correlations, it is necessary to measure the critical crack length, and we were unable to do this.

5. Transformation of the Broken Front of a Crack to a Rectilinear Front. The initial rectilinear front (the straight line Oz) of a flat crack can be transformed to a broken front of the flat crack in the plane Oxz using the discrete-integral criteria of brittle strength for the weakest monolayer of atoms. Indeed, criterion (4.1) is derived for a weak monolayer of atoms, and the plane of this monolayer is perpendicular to the initial rectilinear crack front. We assume that there are two or three such identical layers and they adjoin one another (this assumption is used below in Neuber–Novozhilov averaging of the stress field in the vicinity of the vertices of a broken line). Let, in successive additional loading of the cracked sample, the load reach a critical value. Then, the rectilinear front Oz becomes a broken front of the flat crack (the broken lines $a_0Oa_1a_2a_3a_{00}$ and $a_0Ob_1b_2b_3a_{00}$ in Fig. 5a and b, where the simplest shape of such fronts is given. Apparently, the arrangement of the links of the broken line correlates with the geometric characteristics of the lattice packing: the packing of atoms (particles) can be close (Fig. 5a) or it can correspond to a rectangular lattice (Fig. 5b). The dashed regions in the vicinity of the vertices of the broken line are the regions of averaging after Neuber [13] and Novozhilov [9] [see relation (4.1)], and the diameter of these regions coincides with the grain size for a material with an ideal crystal structure.

In the vicinity of the vertices of the broken line, the estimates of the stress singularity at the corners of wedge-shaped cracks are valid [14]. It is expedient to perform integration in polar coordinates using the modified criteria of brittle strength (4.1). Instead of relation (4.2), we now consider the relation that holds in the vicinity of the vertices of the broken line:

$$\tau_{xy}(r, \varphi, 0) = \tau_\infty + K_{II}A_2(\varphi)/(2\pi)^{1/2}r^{1-\gamma_2}.$$

Here (r, φ) are polar coordinates in the crack plane, and the coordinate origin coincides with one of the vertices of the broken line, $A_2(\varphi)$ is a function with no singularities, such that $A_2(\varphi) = O(1)$, and γ_2 is a parameter [14] that describes singularity. Parihar and Keer [14] obtained this parameter for the problem of shear for a wedge-shaped crack. They established that $\gamma_2 = \gamma_2(\nu)$, where ν is the Poisson's constant. The values of the parameters γ_2 for various ν depending on the cone angle of the wedge 2α are listed in Table 1.

We note that for wedge angles $2\alpha = \pi/3$, $2\pi/3$, $4\pi/3$, and $5\pi/3$, the values of the singularity parameter

966

TABLE 1

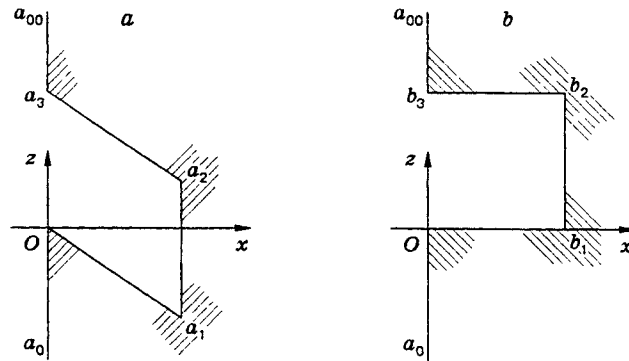| 2α	$\gamma_2 \ (\nu = 0)$	$\gamma_2 \ (\nu = 1/4)$	$\gamma_2 \ (\nu = 1/2)$
$\pi/3$	0.2399	0.2658	0.2986
$\pi/2$	0.2966	0.3285	0.3733
$2\pi/3$	0.3579	0.3861	0.4260
π	0.5	0.5	0.5
$4\pi/3$	0.6994	0.6508	0.5865
$3\pi/2$	0.8146	0.7492	0.6577
$5\pi/3$	0.9093	0.8686	0.8003

Fig. 5

are obtained by interpolation of the results of [14]. These angles correspond to close-packed layers of atoms in the crack plane. In addition, at an arbitrary angle $2\alpha < 2\pi$, the singularity parameter $1 - \gamma_2 < 1$ (see [14] and Table 1). This makes it possible to use the modified discrete–integral criterion (4.1). After obvious calculations, comparison of the orders of magnitude of the quantities shows that, as compared to the rectilinear front of flat cracks $2\alpha = \pi$ and $\gamma_2 = 0.5$, wedge-shaped cracks are: (1) less stable at $2\alpha < \pi$ since $\gamma_2 < 0.5$; (2) more stable at $2\alpha > \pi$ since $\gamma_2 > 0.5$. Hence, the broken front of a flat crack tends to transform to a rectilinear front, and the highest "concentration" of average stresses takes place at $2\alpha = \pi/3$, $2\alpha = \pi/2$, and small ν.

In successive additional loading, when the rectilinear front of a flat crack has a segment corresponding to the weakest atomic layer, the flat crack propagates as follows: (1) when a critical load is attained, the crack propagates locally in this segment by inflection of the front, and a broken front forms; (2) at the same load, additional loading and unloading of interatomic bonds take place in the vicinity of the acute and blunt angles of the broken line, respectively; (3) a new advanced rectilinear front of the crack forms. At the new rectilinear front, the weakest segment is found, and the process occurs again.

Conclusion. It is shown for the first time that interatomic bonds are partially restored in powder compaction at rather moderate pressures. The proposed processing of the experimental strength of the compacts produced is in qualitative agreement with full-scale experiments.

Remark. In Sec. 4, just one version of the theoretical processing of experimental data is proposed since the original system obtained by compaction has a hierarchy of structures. Different approaches can be based on the ideas of [15, 16], where the strength of cracked bodies is described. We believe that the fracture structure depends on the original structure of the material and does not form during fracture [16].

REFERENCES

1. A. B. Mosolov, "Fractal Griffith crack," *Zh. Tekh. Fiz.*, **61**, No. 7, 57–60 (1991).

2. R. V. Gol'dshtein amd A. B. Mosolov, "Cracks with a fractal surface," *Dokl. Akad. Nauk SSSR*, **319**, No. 4, 840–844 (1991).

3. A. B. Mosolov and F. M. Borodich, "Fractal fracture of ductile solids in compression," *Dokl. Ross. Akad. Nauk*, **324**, No. 3, 546–554 (1992).

4. A. D. Zimon, *World of Particles* [in Russian] Nauka, Moscow (1988).

5. E. F. Mikhailov, S. S. Vlasenko, A. A. Kiselev, and T. I. Ryshkevich, "Change of the structure of fractal soot particles under the action of capillary forces: experimental results," *Kolloid Zh.*, **59**, No. 2, 195–203 (1997).

6. T. Sato, "Thermal decomposition of aluminum hydroxides to aluminas," *Thermochim. Acta.*, **88**, 69–84 (1985).

7. T. A. Korneva, T. S. Yusupov, L. G. Lukjanova, and G. M. Gusev, "Thermal analysis of mechanically activated bauxites," in: *Thermal Analysis*: Proc. of the 4th ICTA, Vol. 3, Budapest (1974), pp. 659–664.

8. V. M. Kornev, "Integral criteria for the brittle strength of cracked solids with defects in the presence of vacancies at the tip of a crack. Strength of compacted ceramics-type bodies," *Prikl. Mekh. Tekh. Fiz.*, **37**, No. 5, 168–177 (1996).

9. V. V. Novozhilov, "On the necessary and sufficient criterion of brittle strength," *Prikl. Mat. Mekh.*, **33**, No. 2, 212–222 (1969).

10. K. G. Schmitt-Thomas, *Metallkunde für das Maschinenwesen*, Springer-Verlag (1989).

11. N. H. Macmillan "The ideal strength of solids," in: *Atomistic of Fracture*, R. Latanision and J. R. Pickens (eds.), Plenum Press, New York (1983), pp. 95–164.

12. M. P. Savruk, "Stress intensity factors in cracked solids," in: *Fracture Mechanics and Strength of Materials* [in Russian], Vol. 2, Naukova Dumka, Kiev (1988).

13. H. Neuber, *Kerbspannunglehre: Grunglagen fürGenaue Spannungsrechnung*, Springer-Verlag (1937).

14. K. S. Parihar and L. M. Keer, "Stress singularity at the corner of a wedge-shaped crack or inclusion," *Trans. ASME, Ser. E, J. Appl. Mech.*, **45**, No. 4, 791–796 (1978).

15. V. V. Adishchev and V. M. Kornev, "Method of deriving a brittle strength criterion for cracked solids," *Izv. Vyssh. Uchebn. Zaved., Stroitel'stvo*, No. 7, 41–45 (1997).

16. R. V. Gol'dshtein and N. M. Osipenko, "Destruction and formation of structures," *Dokl. Akad. Nauk SSSR*, **240**, No. 4, 829–832 (1978).